Inorg. Chem. **2005**, *44*, 6277−6283

Molecular Dynamics of a Vanadate−Dipeptide Complex in Aqueous Solution†

Michael Bühl*

Max-Planck-Institut für Kohlenforschung, Kaiser-Wilhelm-Platz 1, D-45470 Mülheim an der Ruhr, Germany

Received May 4, 2005

Static geometry optimizations and Car−Parrinello molecular dynamics simulations with the BP86 density functional, as well as NMR chemical shift calculations at the GIAO-B3LYP level, have been used to assess structure, speciation, and dynamics of aqueous solutions of the vanadate–glycylglycine complex. According to the simulations, this complex should be formulated as five-coordinate, anionic $[VO_2(GlyGly')]^-$ (GlyGly′ = $H_2N–CH_2–C(O)–N–CH_2–CO_2$). The neutral conjugate acid is unstable in water, where it is deprotonated within a few picoseconds. Six-coordinate structural alternatives, $[VO(OH)_2(GlyGly')]^-$, are disfavored energetically and/or entropically. The hydration shell around $[VO_2(GlyGly')]^-$ in water is characterized in terms of suitable pair correlation functions.

Introduction

Interactions between transition metals and proteins are ubiquitous in biochemistry. The fundamental, intrinsic nature of these interactions can be studied in metal complexes with smaller peptides that are unperturbed by the structural and dynamic complexity of the full protein.[1−3] After the discovery of vanadium as an essential ingredient in specific nitrogenases and haloperoxidases,[4] one of the principal areas of the bioinorganic chemistry of vanadium,[5,6] extensive studies have been directed toward such model complexes between vanadate and small peptides.[2,7,8] For vanadate(V) and simple dipeptides with unfunctionalized side chains, requirements for complex formation and further NMR evidence have led to the suggestion that the peptide acts as tridentate ligand, coordinating via the terminal NH_2 function, the deprotonated peptide N atom, and an O atom from the terminal carboxylate group.[7,8] To date, direct structural evidence for these complexes is lacking, although some closely related vanadate(IV)[9] and peroxovanadate(V)[10] derivatives have been characterized by X-ray crystallography, affording strong support for this suggested binding mode.

Density-functional computations of structures, energies, and ^{51}V chemical shifts of complexes **1a** and selected isomers and conjugate bases thereof have confirmed that this particular ligand arrangement is a possible and plausible candidate for the actual species present in aqueous solution.[11a] For neutral Gly−Gly and Gly−Ser[11b] complexes, static geometry optimizations in the gas phase afforded a 6-fold pseudo-octahedral coordination about vanadium with one weakly bound solvent molecule (**1a**), reminiscent of structures of vanadate complexes with other polydentate N and O donors in the solid.[12] Upon deprotonation of the neutral complex, this weakly bound water molecule detached from

* E-mail: buehl@mpi-muelheim.mpg.de. Fax: + (0)208-306-2996.

† Dedicated to Prof. Dr. Michele Parrinello on the occasion of his 60th birthday.

(1) For recent examples see: (a) Barnard, P. J.; Levina, A.; Lay, P. A. *Inorg. Chem.* **2005**, *44*, 1044−1053. (b) Huang, H.; Chaudhary, S.; Van Horn, J. D. *Inorg. Chem.* **2005**, *44*, 813−815. (c) Tesfai, T. M.; Green, B. J.; Margerum, D. W. *Inorg. Chem.* **2004**, *43*, 6726−6733, and references therein.

(2) Durupthy, O.; Coupé, A.; Tache, L.; Rager, M.-N.; Maquet, J.; Coradin, T.; Stenou, N.; Livage, J. *Inorg. Chem.* **2004**, *43*, 2021−2030.

(3) Kozlowski, H.; Bal, W.; Dyba, M.; Kowalik-Jankowska, T. *Coord. Chem. Rev.* **1999**, *184*, 319−346.

(4) Butler, A.; Baldwin, A. H. *Struct. Bonding* **1997**, *89*, 109−132.

(5) (a) Crans, D. C. In *Metal Ions in Biological Systems*; Sigel, H., Sigel, A., Eds.; Marcel Dekker: New York, 1995; Vol. 31, pp 147−210. (b) *Vanadium Compounds - Chemistry, Biochemistry, and Therapeutic Applications*; Tracey, A. S., Crans, D. C., Eds.; ACS Symposium Series 711; American Chemical Society: Washington, DC, 1998.

(6) Rehder, D. *Inorg. Chem. Commun.* **2003**, *6*, 604−617.

(7) (a) Rehder, D. *Inorg. Chem.* **1988**, *27*, 4312−4316. (b) Crans, D. C.; Holst, H.; Keramidas, A. D.; Rehder, D. *Inorg. Chem.* **1995**, *34*, 2524−2534. (c) Fritzsche, M.; Elvingston, K.; Rehder, D.; Pettersson, L. *Acta Chem. Scand.* **1997**, *51*, 483−491.

(8) (a) Jaswal, J. S.; Tracey, A. S. *Can. J. Chem.* **1991**, *69*, 1600−1607. (b) Jaswal, J. S.; Tracey, A. S. *J. Am. Chem. Soc.* **1993**, *115*, 5600−5607. (c) Einstein, F. W. B.; Batchelor, R. J.; Angus-Dunne, S. J.; Tracey, A. S. *Inorg. Chem.* **1996**, *35*, 1680−1684.

(9) $[VO(GlyGly')(phen)]$ (phen = 1,10-phenanthroline): Tasiopoulos, A. J.; Troganis, A. N.; Deligiannakis, Y.; Evangelou, A.; Kabanos, T. A.; Woollins, J. D.; Slawin, A. *J. Inorg. Biochem.* **2000**, *79*, 159−166.

(10) $[VO(O_2)(GlyGly')]$: ref 8c.

(11) (a) Bühl, M. *J. Comput. Chem.* **1999**, *20*, 1254−1261. (b) Bühl, M. *J. Inorg. Biochem.* **2000**, *80*, 137−139.

10.1021/ic050694i CCC: $30.25
Published on Web 08/10/2005

Chart 1

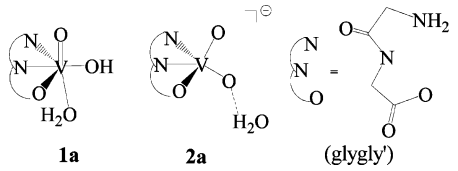

the metal, leaving the latter five-coordinated **2a** (Chart 1). This result pointed to the interesting possibility that the coordination geometry about vanadium could be dependent on, and tunable by, the pH value.

To what extent are these gas-phase results transferable to physiological conditions, that is, aqueous solution at pH 7? Structures, properties, and dynamics on the picosecond time scale can now be reliably studied by density-functional based molecular dynamics (MD) simulations. The Car−Parrinello MD (CPMD) approach[13] has proven to be particularly well suited for this purpose.[14] We have previously applied this method to simulate structures and ^{51}V chemical shifts of simple vanadate and peroxovanadate complexes in aqueous solution,[15] including imidazole as a biogenic histidine model, and of other transition-metal complexes.[16] In the present paper, these studies are extended to the parent vanadate−glycylglycine complex, calling special attention to the coordination environment about the metal and to the protonation state of the complex.

Computational Details

Stationary points were optimized with the Gaussian suite of programs[17,18] at the BP86/AE1 level, i.e., employing the exchange and correlation functionals of Becke[19] and Perdew,[20] respectively, together with a fine integration grid (75 radial shells with 302 angular points per shell) and employing the augmented all-electron Wachters basis[21] on V (8s7p4d, full contraction scheme 62111111/3311111/ 3111) and the 6-31G* basis[22] on all other elements. This and comparable DFT levels have proven to be quite successful for transition-metal compounds and are well suited for the description of structures, energies, barriers, etc.[23] The nature of the stationary points was verified by computations of the harmonic frequencies at that level. Transition states were characterized by a single imaginary frequency, and visual inspection of the corresponding vibrational modes ensured that the desired minima were connected. The computed harmonic frequencies were used to evaluate zero-point energies (ZPEs), as well as enthalpic and entropic contributions. Single-point energy calculations were performed for the BP86/AE1 geometries at the BP86/AE1+ level, i.e., with the same basis augmented with diffuse functions on C, N, and O.[24] The basis sets were the same as those used in ref 15a. Calculations in a polarizable continuum were effected using the parameters of water and the implementation[25] in Gaussian 03.[18]

Geometries were reoptimized using the density-functional based Car−Parrinello scheme[13], as implemented in the CPMD program,[26] until the maximum gradient was less than 5×10^{-4} au (denoted CP-opt). The BP86 functional was employed together with norm-conserving pseudopotentials generated according to the Troullier and Martins procedure[27] and transformed into the Kleinman−Bylander form.[28] For vanadium, the semicore (or small-core) pseudopotential from ref 15b was employed. Periodic boundary conditions were imposed using a cubic supercell with a box size of 13.0 Å. Kohn−Sham orbitals were expanded in plane waves up to a kinetic energy cutoff of 80 Ry.[29] For the complexes in vacuo, Car−Parrinello molecular dynamics simulations were performed starting from the equilibrium structure using a fictitious electronic mass of 600 au and a time step of 0.121 fs. Unconstrained simulations (NVE ensemble) were performed over 1.5 ps at ca.

(12) Bashirpoor, M.; Schmidt, H.; Schulzke, C.; Rehder, D. *Chem. Ber./Recl.* **1997**, *130*, 651−657.
(13) Car, R.; Parrinello, M. *Phys. Rev. Lett.* **1985**, *55*, 2471−2474.
(14) For selected reviews see: (a) Tuckerman, M. E. *J. Phys.: Condens. Matter* **2002**, *14*, R1297−R1355. (b) Tse, J. S. *Annu. Rev. Phys. Chem.* **2002**, *53*, 249−290. (c) Carloni, P.; Röthlisberger, U.; Parrinello, M. *Acc. Chem. Res.* **2002**, *35*, 455−464.
(15) (a) Bühl, M.; Parrinello, M. *Chem.−Eur. J.* **2001**, *7*, 4487−4494. (b) Bühl, M.; Schurhammer, R.; Imhof, P. *J. Am. Chem. Soc.* **2004**, *126*, 3310−3320.
(16) (a) Bühl, M.; Mauschick, F. T.; Terstegen, F.; Wrackmeyer, B. *Angew. Chem., Int. Ed.* **2002**, *41*, 2312−2315. (b) Bühl, M.; Mauschick, F. *Phys. Chem. Chem. Phys.* **2002**, *4*, 5508−5514. (c) Bühl, M. *J. Phys. Chem. A* **2002**, *106*, 10505-10509. (d) Bühl, M.; Grigoleit, S.; Kabrede, H.; Mauschick, F. T. *Chem.−Eur. J.*, in press.
(17) Frisch, M. J.; Trucks, G. W.; Schlegel, H. B.; Scuseria, G. E.; Robb, M. A.; Cheeseman, J. R.; Zakrzewski, V. G.; Montgomery, J. A.; Stratman, R. E.; Burant, J. C.; Dapprich, S.; Millam, J. M.; Daniels, A. D.; Kudin, K. N.; Strain, M. C.; Farkas, O.; Tomasi, J.; Barone, V.; Cossi, M.; Cammi, R.; Mennucci, B.; Pomelli, C.; Adamo, C.; Clifford, S.; Ochterski, J.; Petersson, G. A.; Ayala, P. Y.; Cui, Q.; Morokuma, K.; Malick, D. K.; Rabuck, A. D.; Raghavachari, K.; Foresman, J. B.; Cioslowski, J.; Ortiz, J. V.; Baboul, A. G.; Stefanov, B. B.; Liu, C.; Liashenko, A.; Piskorz, P.; Komaromi, I.; Gomperts, R.; Martin, R. L.; Fox, D. J.; Keith, T.; Al-Laham, M. A.; Peng, C. Y.; Nanayakkara, A.; Gonzalez, C.; Challacombe, M.; Gill, P. M. W.; Johnson, B. G.; Chen, W.; Wong, M. W.; Andres, J. L.; Gonzales, C.; Head-Gordon, M.; Replogle, E. S.; Pople, J. A. *Gaussian 98;* Gaussian, Inc.: Pittsburgh, PA, 1998.
(18) Frisch, M. J.; Trucks, G. W.; Schlegel, H. B.; Scuseria, G. E.; Robb, M. A.; Cheeseman, J. R.; Montgomery, J. A., Jr.; Vreven, T.; Kudin, K. N.; Burant, J. C.; Millam, J. M.; Iyengar, S. S.; Tomasi, J.; Barone, V.; Mennucci, B.; Cossi, M.; Scalmani, G.; Rega, N.; Petersson, G. A.; Nakatsuji, H.; Hada, M.; Ehara, M.; Toyota, K.; Fukuda, R.; Hasegawa, J.; Ishida, M.; Nakajima, T.; Honda, Y.; Kitao, O.; Nakai, H.; Klene, M.; Li, X.; Knox, J. E.; Hratchian, H. P.; Cross, J. B.; Bakken, V.; Adamo, C.; Jaramillo, J.; Gomperts, R.; Stratmann, R. E.; Yazyev, O.; Austin, A. J.; Cammi, R.; Pomelli, C.; Ochterski, J. W.; Ayala, P. Y.; Morokuma, K.; Voth, G. A.; Salvador, P.; Dannenberg, J. J.; Zakrzewski, V. G.; Dapprich, S.; Daniels, A. D.; Strain, M. C.; Farkas, O.; Malick, D. K.; Rabuck, A. D.; Raghavachari, K.; Foresman, J. B.; Ortiz, J. V.; Cui, Q.; Baboul, A. G.; Clifford, S.; Cioslowski, J.; Stefanov, B. B.; Liu, G.; Liashenko, A.; Piskorz, P.; Komaromi, I.; Martin, R. L.; Fox, D. J.; Keith, T.; Al-Laham, M. A.; Peng, C. Y.; Nanayakkara, A.; Challacombe, M.; Gill, P. M. W.; Johnson, B.; Chen, W.; Wong, M. W.; Gonzalez, C.; Pople, J. A. *Gaussian 03*; Gaussian, Inc.: Wallingford, CT, 2004.
(19) Becke, A. D. *Phys. Rev. A* **1988**, *38*, 3098−3100.
(20) Perdew, J. P. *Phys. Rev. B* **1986**, *33*, 8822−8824. Perdew, J. P. *Phys. Rev. B* **1986**, *34*, 7406.
(21) (a) Wachters, A. J. H. *J. Chem. Phys.* **1970**, *52*, 1033−1036. (b) Hay, P. J. *J. Chem. Phys.* **1977**, *66*, 4377−4384.
(22) (a) Hehre, W. J.; Ditchfield, R.; Pople, J. A. *J. Chem. Phys.* **1972**, *56*, 2257−2261. (b) Hariharan, P. C.; Pople, J. A. *Theor. Chim. Acta* **1973**, *28*, 213−222.
(23) See, for instance: Koch, W.; Holthausen, M. C. *A Chemist's Guide to Density Functional Theory*; Wiley-VCH: Weinheim, Germany, 2000, and the extensive bibliography therein.
(24) Clark, T.; Chandrasekhar, J.; Spitznagel, G. W.; Schleyer, P. v. R. *J. Comput. Chem.* **1983**, *4*, 294−301.
(25) (a) Miertus, S.; Scrocco, E.; Tomasi, J. *Chem. Phys.* **1981**, *55*, 117−129. (b) Mennucci, B.; Tomasi, J. *J. Chem. Phys.* **1997**, *106*, 5151−5158. (c) Barone, V.; Cossi, M.; Tomasi, J. *J. Chem. Phys.* **1997**, *107*, 3210−3221.
(26) *CPMD*, version 3.7.0; Copyright IBM Corp., 1990−2001; Copyright MPI für Festkörperforschung Stuttgart, 1997−2001.
(27) Troullier, N.; Martins, J. L. *Phys. Rev. B* **1991**, *43*, 1993−2006.
(28) Kleinman, L.; Bylander, D. M. *Phys. Rev. Lett.* **1982**, *48*, 1425−1428.
(29) The notations AE1 and CP-opt thus denote two different approximations for constructing the Kohn−Sham wave function, namely, one based on an all-electron basis set moving with the atoms and the other on atomic pseudopotential cores swimming in a sea of periodic plane waves.

300 K, the first 0.5 ps of which was taken for equilibration. For the aqueous solutions, the boxes were filled with 60 additional water molecules. To increase the time step, hydrogen was substituted with deuterium. The systems were equilibrated for 0.5 ps maintaining a temperature of 300 (±50) K and were then propagated without constraints for 1−4.5 ps.

Magnetic shieldings were computed for equilibrium structures and for snapshots along the trajectories employing gauge-including atomic orbitals (GIAOs)[30] and the B3LYP[31] hybrid functional together with basis AE1+. Snapshots were taken every 20 fs over the last 1 ps. No periodic boundary conditions were employed, and solvent water molecules were not included specifically but in the form of point charges employing values of −0.9313 and +0.4656 for O and H atoms, respectively, as obtained for a single water molecule from natural population analysis (NPA)[32] at the B3LYP/6-31G* level (water molecules from the six adjacent boxes were also included as point charges, cf. the procedure in ref 15a). These computations were carried out with the Gaussian 98 program package.[17] Chemical shifts are reported relative to VOCl3 and are optimized or simulated at the same respective level (σ-values of −2319 and −2264 ppm employing BP86/AE1 and CP-opt geometries, respectively, and −2292 ppm for a CPMD simulation averaged over 1 ps). ^{15}N chemical shifts are reported relative to nitromethane (σ-values of −94.2 and −128.5 ppm for CP-opt and CPMD level, respectively). After 1 ps of sampling, the mean ^{51}V and ^{15}N chemical shifts were typically converged to within ca. 5 and 0.5 ppm, respectively.

Results and Discussion

Structures and Dynamics. As a first step, a CPMD simulation was performed for neutral **1a** in the gas phase, starting from the fully optimized minimum. The geometrical parameters optimized with the periodic plane-wave method are very similar to those derived previously with nonperiodic computations and Gaussian-type basis sets,[11a] except for the V−O bond to the coordinated water molecule. This bond is notably longer in the BP86/CP-opt than in the BP86/AE1 geometry (2.686 Å vs 2.525 Å), betraying the rather weak binding of this ligand. In fact, the computed dissociation energy for the process **1a** → **3** + H_2O is very low (4.0 kcal/mol at the BP86/CP-opt level). This value is even smaller than that of typical systems involving hydrogen-bonded water molecules (e.g., 4.4 kcal/mol in the water dimer at the same level). It is therefore not surprising that **1a** is not stable in a CPMD run in the gas phase but rearranges spontaneously to isomer **1b**, in which the water molecule is hydrogen-bonded to another ligand (the terminal NH_2 group of the GlyGly moiety in this case; see Chart 2). When fully optimized, this isomer is lower in energy than **1a** by 1.0 kcal/mol at the BP86/CP-opt level. Conceivably, there exists a whole set of related clusters with water attached to different positions at the VO(OH)(GlyGly′) core, presumably all with similar energies. Thus, six-coordinate **1a** is not only kinetically but also thermodynamically unstable in the gas phase, where it rearranges to a microsolvated, five-coordinate species.

Chart 2

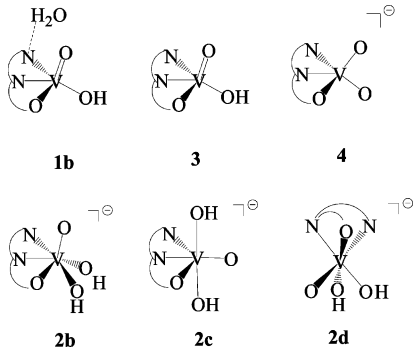

The situation may be different in the bulk, however. For other vanadate complexes with datively bonded ligands, notably in the $[VO(O_2)_2L]^-$ series (L = H_2O, imidazole), the simulations have revealed a notable V−L bond contraction upon going from the gas phase into the aqueous solution (up to 0.095 Å for imidazole).[15] This observation is indicative of a considerable reinforcement of this otherwise weak V−L bond. If a similar strengthening would occur in the dipeptide complex, then hexacoordinate **1a** might be stable in water. Indeed, during the first few hundred femtoseconds of a CPMD simulation of aqueous **1a**, such a slight contraction of the V−OH_2 distance seemed to be occurring. After ca. 0.6 ps, however, the water molecule was expelled from the complex and drifted off into the bulk solvent (see the corresponding V−O distance in Figure 1, full line at the upper left) affording aqueous **3**.

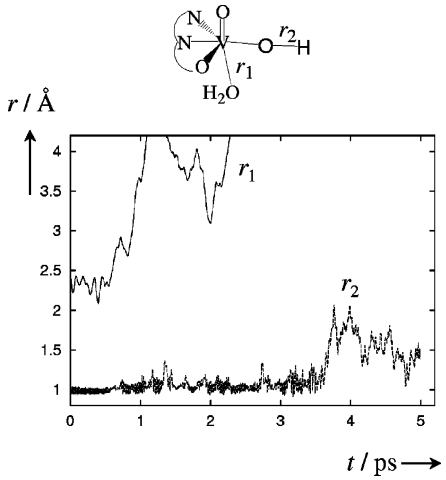

Figure 1. Evolution of selected bond distances in a CPMD simulation of **1a** in water.

When the simulation was repeated from the same starting configuration but with the V(OH) moiety deprotonated, the water molecule detached immediately from the metal and trailed off into the bulk with the V−OH_2 distance exceeding 3 Å after only 0.13 ps. Thus, both neutral and deprotonated species afford basically the same pentacoordinate ligand environment about vanadium.

When the simulation of **3** in water was continued for a total of ca. 3.7 ps, the proton of the hydroxyl ligand was

(30) (a) Ditchfield, R. *Mol. Phys*. **1974**, *27*, 789. (b) Wolinski, K.; Hinton, J. F.; Pulay, P. *J. Am. Chem. Soc*. **1990**, *112*, 8251. (c) Cheeseman, J. R.; Trucks, G. W.; Keith, T. A.; Frisch, M. J. GIAO-DFT Implementation. *J. Chem. Phys.* **1996**, *104*, 5497.
(31) Lee, C.; Yang, W.; Parr, R. G. *Phys. Rev. B* **1988**, *37*, 785−789.
(32) Reed, A. E.; Curtiss, L. A.; Weinhold, F. *Chem. Rev*. **1988**, *88*, 899−926.

Table 1. Energies (kcal/mol) of $[VO(OH)_2(GlyGly')]^-$ Isomers Relative to $[VO_2(GlyGly')]^- + H_2O$

level[a]	2b	2c	2d	TS2b4
BP86/AE1+	0.9	9.0	2.0	11.2
BP86/CP-opt	2.7	8.3	3.8	
B3LYP/AE1+	3.5	11.6	4.2	16.8
BP86/AE1+ +ZPE[b]	2.5	10.3	4.1	11.2
ΔH^{298}(BP86/AE1+)[b]	2.2	9.4	2.9	9.7
ΔG^{298}(BP86/AE1+)[b]	13.7	20.3	14.4	21.5
PCM(BP86/AE1+)[c]	−1.0	5.4	−0.6	8.9
PCM(B3LYP/AE1+)[c]	2.0	8.1	1.9	14.8

[a] Single-point energies for BP86/AE1 optimized geometries, except for BP86/CP-opt entry. [b] Vibrational and thermal corrections evaluated at the BP86/AE1 level. [c] Polarizable continuum employing the parameters of water.

transferred to a water molecule from the solvent under formation of a $[VO_2(GlyGly')]^- \cdot H_3O^+$ contact ion pair. This process can be followed in the time evolution of the VO−H distance in Figure 1 (dotted line labeled r_2). The contact ion pair was stable for at least another picosecond. Clearly, only limited conclusions can be drawn from such a singular event. Its rapid occurrence in an unconstrained MD run, however, strongly suggests that the neutral complex **3** with its VO(OH) moiety is indeed a strong acid, and if it could be prepared and isolated in pure form, then it would ionize to a large extent in water. In a buffered solution at pH 7, it is very likely that the proton is consumed by the buffer, yielding anionic $[VO_2(GlyGly')]^-$ (**4**). Thus, these simulations are completely in accord with the formulation of vanadate−peptide complexes as monoanions at pH 7.

Apparently, an intact water molecule cannot bind to five-coordinate vanadate−peptide complexes. To test if hexa-coordination is possible at all in these species, an extensive search for $[VO(OH)_2(GlyGly')]^-$ isomers was conducted. These species are, formally, "OH activated" products of water addition to **4** and have recently been invoked as possible structures.[2] Optimizations were started in vacuo from a larger number of initial ligand configurations and converged to three distinct minima, namely, **2b** and **2c** with the same *mer* configuration of the dipeptide ligand as encountered in all minima so far, and **2d** with a *fac* orientation of this ligand (Chart 2). The relative energies of these species, collected in Table 1 with respect to separated **4** + H_2O, depend somewhat on the density functional employed. In the gas phase, **2b**−**d** are always less stable than the separated reactants by at least ca. 1 kcal/mol. Zero-point, enthalpic, and, in particular, entropic corrections additionally disfavor the six-coordinate complexes, which should, thus, not be thermodynamically stable in the gas phase (see ΔH and ΔG values in Table 1). The *mer* isomer **2c** with peptide N and terminal oxo atoms in the trans position is already strongly disfavored energetically and is unlikely to be populated to any noticeable extent.

Relative energies may change in solution, however, where the entropy gain due to an increase in particle number also tends to be less pronounced than in the gas phase. Embedding the structures that were optimized in vacuo in a polarizable continuum (employing the dielectric constant of water) reduces the energetic separation between the isomers somewhat. At the PCM(BP86/AE1+) level, the six-coordinate

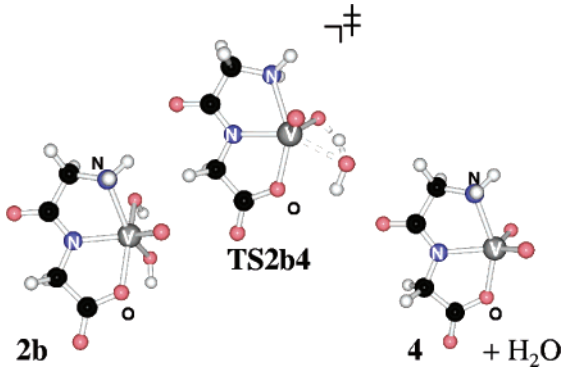

Figure 2. *mer*-$[VO(OH)_2(GlyGly')]^-$ (**2b**, left), together with the transition state for water elimination (**TS2b4**, middle) and the resulting five-coordinate $[VO_2(GlyGly')]^-$ (**4**, right), BP86/AE1 optimized.

species **2b** and **2d** are even slightly more stable than the five-coordinated **4** + H_2O. When the corresponding solvation energies (i.e., the differences between BP86/AE1+ and PCM data) are added to the gas phase, ΔH values for **2b** and **2d** are almost isenthalpic with **4** + H_2O. As entropy is expected to disfavor these six-coordinate species significantly, it is unlikely that they will play a significant role in the speciation of the vanadate−GlyGly complex, even more so for *mer*-**2c** which is much higher in energy throughout.

It is interesting, however, that the energetic separation between *mer*-**2b** and *fac*-**2d** is so small (less than 1 kcal/mol at most levels). Transition-metal complexes involving tridentate dipeptide ligands (such as glycylglycine in this study) are quite common, and in all cases that have been structurally characterized, a *mer* configuration with an essentially planar $\{N_2OM\}$ moiety (M = metal) has been found.[9,10,33] Our results for the six-coordinate vanadate complexes suggest that *fac* isomers need not be excessively high in energy and might actually be accessible with the appropriate co-ligands.

The structure of *mer*-**2b** is interesting; even though the optimization started from an octahedral arrangement of the donor atoms about vanadium, the final structure has a different coordination geometry, with the terminal oxo and the two OH groups above and below the $\{N_2OV\}$ plane, respectively (Figure 2). This arrangement closely resembles that of the related peroxo complex $[VO(O_2)(GlyGly')]^-$, from which **2b** is formally derived by reduction of the peroxo ligand. **2b** is stable in CPMD runs in the gas phase (4 ps) and in water (1.5 ps). No quantitative information concerning the relative stability of **2b** and **4** in water can be obtained from these unconstrained simulations. In principle, the change in free energy can be calculated via thermodynamic

(33) For some typical examples with metals other than V see the following: (a) $[Cr(GlyGly')_2]^-$: Murdoch, C. M.; Cooper, M. K.; Hambley, T. W.; Hunter, W. N.; Freeman, H. C. *J. Chem. Soc., Chem. Commun.* **1986**, 1329−1331. (b) [Co(GlyGly')(en)(NCS)]: Solujic, L. R.; Herak, R.; Prelesnik, B.; Celap, M. B. *Inorg. Chem.* **1985**, *24*, 32−37. (c) $[Ni(GlyGly')_2]^{2-}$: Freeman, H. C.; Guss, J. M. *Acta Crystallogr., Sect. B* **1987**, *34*, 2451. (d) [ReO(GlyGly'){*o*-C_6H_4(O)-(PPh_2)}]: Nock, B.; Maina, T.; Tisato, F.; Raptopoulou, C. P.; Terzis, A.; Chiotellis, E. *Inorg. Chem.* **2000**, *39*, 5197−5202. (e) [Ru(GlyGly')(PPh_3)$_2$(MeOH)]: Sheldrick, W. S.; Exner, R. *Inorg. Chim. Acta* **1991**, *184*, 119−125.

Table 2. Chemical Shifts (GIAO-B3LYP/AE1+ Level) of Vanadate−Glycylglycine Complexes

level[b]	**3**	**4**	**2b**	**2d**	exptl[a]
CP-opt					
V	−523	−637	−514	−477	
N^{p} [c]	−117	−167	−125	−115	
NH_2	−319	−332	−299	−303	
CMPD/D_2O					
V	−564	−627	−518		−505
N^{p}	−155	−190	−159		−202
NH_2	−345	−355	−324		−344

[a] Exptl ^{51}V data from ref 8a and ^{14}N data for Ala−Gly complex from ref 2. [b] Source of geometries: CP-opt, static equilibrium values in the gas phase; CPMD/D_2O, dynamic average in water. [c] N^{p}: peptide nitrogen atom.

integration of the constraint mean force along a predefined reaction coordinate connecting both forms.[34] The large number of necessary constrained MD runs and the long simulation times required for sufficient numerical precision would make such a procedure a formidable task beyond the scope of the present paper.

From the energetic data in Table 1, a noticeable preference of five-coordinate **4** over *mer*-**2b** is predicted. If both are present in an equilibrium mixture, then interconversion between them is expected to be rapid, at least on the NMR time scale. To support this notion, one possible transition state for this interconversion has been located (**TS2b4**, Figure 2).[35] This structure describes the transfer of the proton from one OH group onto the O atom of the other. Depending on the theoretical level, a barrier between ca. 9 and 17 kcal/mol relative to separated **4** + H_2O is computed on the potential energy surfaces (Table 1), which increases somewhat to ca. 22 kcal/mol at the free energy surface. The barrier relative to **2b** is considerably smaller, ca. 8−13 kcal/mol (see differences between entries for **2b** and **TS2b4** in Table 1). Quite possibly, intermolecular assistance by water molecules from the solvent may lower this barrier even further, thereby facilitating equilibration between **2b** and **4** in solution. Speciation between both forms would thus be difficult to detect in the NMR spectra, which would show averaged signals.

Chemical Shifts. Both MD simulations and energetic data presented so far favor the formulation of the vanadate−glycylglycine complex as an anionic, five-coordinate species, rather than as a neutral or six-coordinate form. Comparison of computed and experimental chemical shifts could furnish further information on the possible composition of an equilibrium mixture. ^{51}V NMR spectroscopy is an important analytical tool for diamagnetic vanadium complexes in general[36] and for the vanadate−peptide complexes in particular. Salient $\delta(^{51}V)$ and $\delta(^{14}N)$ data are summarized in Table 2. As ^{14}N chemical shifts have not been reported for the actual vanadate complex with Gly−Gly, experimental values are taken from the closely related Ala−Gly complex.[2] It is unlikely that this minor modification at the peptide chain rather far from the metal would affect the nuclei in the coordination sphere of the latter significantly. Experimental ^{17}O NMR data on such complexes are sparse; the computed ^{13}C magnetic shieldings are unremarkable and of little diagnostic value, so results for these nuclei are not given.

The ^{51}V chemical shifts computed for neutral **3** and for the six-coordinate anions **2b** and **2d** appear to fit very well to experimental values. In contrast, that of anionic **4** tends to be too strongly shielded both in the static equilibrium structure and in the dynamic average in aqueous solution (see CP-opt and CPMD entries in Table 2). However, the error for **4**, e.g., 125 ppm for the simulation in water, falls within the typical accuracy for theoretical $\delta(^{51}V)$ values in general,[37] and other vanadates and peroxovanadates modeled in aqueous solution so far have displayed a similar upfield shift in $\delta(^{51}V)$ with respect to experimental values.[15] Thus, the computed metal shifts are not conclusive for distinguishing between these species.

The ^{14}N chemical shifts turn out to be mildly sensitive to protonation state and coordination number, in particular, the resonance of the peptide N atom (N^{p} in Table 2). The $\delta(^{14}N)$ data are also more prone to dynamic and solvation effects, which tend to make the ^{14}N resonances more shielded (which is to a large extent a consequence of the pronounced deshielding in the standard upon thermal averaging). Among the ^{14}N chemical shifts modeled in aqueous solution, those for **4** fit best experimental values with deviations of a little over 10 ppm, an excellent agreement for this property. Larger discrepancies, ca. 40−50 ppm for N^{p}, are found for **3** and **2b** (and are also expected for **2d**, which has not been modeled in solution), which would argue against the exclusive presence or predominance of one of these forms. Even though the exact composition of the vanadate−glycylglycine equilibrium mixture cannot be predicted with confidence on these grounds, the computed NMR data are consistent with five-coordinate **4** being the principal component of such a mixture.

Solvation effects on the chemical shifts are fairly small, in particular, the direct one arising from the response of the electronic wave function of the solute to the presence of the surrounding solvent.[38] This effect can be estimated by averaging the CPMD snapshots from the simulation in water, employing only the coordinates of the solute thereby omitting the solvent. For **4**, this procedure results in changes of the δ-values relative to the CPMD/D_2O entries in Table 2 of +35, −4, and +1 ppm for V, N^{p}, and NH_2 nuclei, respectively. These are indeed small changes.

The small thermal and solvation effects on these isotropic averages did not result from compensation of larger opposing changes in the individual tensor components. The latter are

(34) For an example involving histidine see: Ivanov, I.; Klein, M. *J. Am. Chem. Soc.* **2002**, *124*, 13380−13381.

(35) The conformation of the CH_2NH_2 bridge in **TS2b4** differs from that of the reactant **2b**; for the latter, no other conformer than that depicted in Figure 2 could be located.

(36) See, for instance: Rehder, D. In *Transition Metal Nuclear Magnetic Resonance*; Pregosin, P. S., Ed.; Elsevier: Amsterdam, 1991; pp 1−58.

(37) (a) Bühl, M.; Hamprecht, F. A. *J. Comput. Chem.* **1998**, *119*, 113−122. (b) Grigoleit, S.; Bühl, M. *Chem.−Eur. J.* **2004**, *10*, 5541−5552. It should be noted that such an error is relatively small compared to the total chemical shift range of ^{51}V, which covers many thousands of parts per million.

(38) As opposed to the indirect effect stemming from the change in geometrical parameters upon solvation.

Table 3. NMR Tensor Components[a] and Geometrical Parameters (Distances in Å)[b] of **4**[c]

property		CP-opt	CPMD/D_2O
^{51}V	δ_{11}	340	354
	δ_{22}	256	256
	δ_{33}	−595	−611
$^{14}N^{P}$ [d]	δ_{11}	90.9	97.5
	δ_{22}	−9.0	−9.2
	δ_{33}	−82.0	−88.3
$^{14}NH_2$	δ_{11}	33.8	25.5
	δ_{22}	−2.3	−1.6
	δ_{33}	−31.4	−23.9
$r(V-O^1)$		1.628	1.628 (15)
$r(V-O^2)$		1.633	1.662 (69)
$r(V-O^3)$		1.941	1.961 (37)
$r(V-N^P)$		2.053	2.047 (38)
$r(V-NH_2)$		2.195	2.122 (41)

[a] Traceless representation, given in ppm, relative to the isotropic average (GIAO-B3LYP/AE1+ level for BP86 optimized or simulated structures). Tensor orientations: for the ^{51}V tensor, the vector along δ_{11} forms angles of 164° and 75° with the $V-O^1$ and $V-O^2$ bonds, respectively, and the vector along δ_{33} forms angles of 78° and 157°, respectively, with these bonds; for the N^P tensor, the vector along δ_{11} forms angles of 128° and 81° with the N−C(O) and $N-C(H_2)$ bonds, respectively, and the vector along δ_{33} forms almost identical angles of ca. 64° with these bonds. [b] For labeling of O atoms see Figure 3. [c] Static equilibrium values in the gas phase and dynamic averages in aqueous solution. [d] N^P: peptide nitrogen atom.

summarized in Table 3 together with salient geometrical parameters, for future reference.

Solution Structure. Finally, it is instructive to analyze the hydration shell around the vanadate−peptide complex. An analysis based on suitable pair correlation (or radial distribution) functions $g(r)$,[39] obtained from the CPMD simulation of aqueous **4**,[40] is presented in Figure 3. These functions are computed between selected heteroatoms from the ligands about vanadium and the O atoms of the surrounding solvent molecules. Specific interactions between these atoms manifest themselves in $g(r)$ values exceeding the isotropic average of 1 (which corresponds to a completely random distribution). Because of the short sampling time of about 2 ps, the pair correlation functions in Figure 3 show a substantial amount of noise, but a number of qualitative features are apparent: The shortest and most frequent contacts with water molecules are found for the terminal oxo atoms at vanadium ($O^{1,2}$) and the noncoordinated O atom from the carboxylate group (O^5) (see top and bottom, respectively, of Figure 3). In both cases, the first maximum in $g(r)$ appears at $r \approx 2.8$ Å, indicative of strong O···H−O hydrogen bonds, and the integral $n_O(r)$ over this maximum, that is, the average number of water molecules in that area, as well as the maximum $g(r)$ value itself, is between 1 and 2. For comparison, in the $g_{OO}(r)$ curve of liquid water, the first peak appears at $r = 2.73-2.88$ Å, with $g > 2.6$.[41]

In comparison to the terminal carboxylate O atom (O^5), the hydration shell around the carbonyl O atom in the peptide

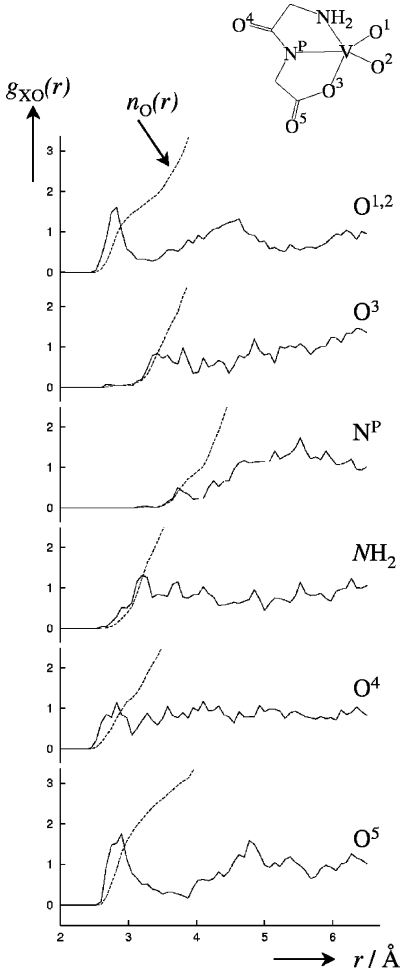

Figure 3. Simulated pair correlation functions $g_{XO}(r)$ in aqueous solution of **4** between designated X and O atoms from the solvent (solid lines) and $n_O(r) = \rho\int g(r)4\pi r^2\,dr$ (dashed lines), which integrates to the total number of O atoms in a sphere with radius r around X.

bond (O^4 in Figure 3) is less pronounced, as the corresponding maximum in $g(r)$ is smaller and appears at a slightly larger r-value. Even weaker interactions with the solvent are apparent for the carboxylate O atom that is coordinated to the metal and for the peptide nitrogen atom (O^3 and N^P, respectively, in Figure 3). The N terminus of the dipeptide acts as a hydrogen-bond donor to the solvent, and the notable peak at $r \approx 3.2$ Å in the corresponding pair correlation function (NH_2 in Figure 3) encompasses such N−H···O linkages.

There is thus an interesting variability in the interaction with the solvent for the various electronegative heteroatoms, which reflects the spatial accessibility of the latter rather than expectations based on electrostatic arguments (e.g., according to natural population analysis[32] at the BP86/AE1+ level, all O and N^P atoms have similar charges between −0.60*e* and −0.68*e*). These results are further testimony to the usefulness of ab initio or DFT-based MD simulations as a means of

(39) For the definition of the pair correlation function see, for example: Allen, M. P.; Tildesley, D. J. *Computer Simulation of Liquids*; Clarendon Press: Oxford, New York, 1987.

(40) The coordination environment of the metal in **4** is best described as a distorted trigonal bipyramid, with N^P, O^1, and O^2 spanning the equatorial plane. As a consequence of the GlyGly′ "bite angle", the $N(H_2)-V-O^3$ bond angle through the apexes is reduced from the ideal value of 180° to 151° (BP86/AE1).

(41) For recent experiments see: (a) Hura, G.; Sorensen, J. M.; Glaeser, R. M.; Head-Gordon, T. *J. Chem. Phys.* **2000**, *113*, 9140−9148. (b) Hura, G.; Sorensen, J. M.; Glaeser, R. M.; Head-Gordon, T. *J. Chem. Phys.* **2000**, *113*, 9149−9161. For recent DFT results see: Vande-Vondele, J.; Mohamed, F.; Krack, M.; Hutter, J.; Sprik, M.; Parrinello, M. *J. Chem. Phys.* **2005**, *122*, 14515.

obtaining insights into the detailed structure and dynamics of the solvation shell around complex solutes.

Conclusion

Static DFT optimizations, Car−Parrinello MD simulations, and NMR chemical shift calculations have been used to assess structure, speciation, and dynamics of the vanadate−glygylglycine complex in aqueous solution. Among the structural candidates considered, neutral $[VO(OH)(H_2O)(GlyGly')]$ (**1a**) is unstable in water, where it spontaneously expels the weakly bound water ligand and ionizes rapidly, affording five-coordinate $[VO_2(GlyGly')]^-$ (**4**). The computed ^{51}V and, in particular, ^{14}N chemical shifts of **4** agree reasonably well with experimental data and are thus entirely compatible with this formulation. *mer*-$[VO(OH)_2(GlyGly')]^-$ (**2b**) is the most stable and, thus, the most promising candidate among possible six-coordinate anionic alternatives. Water elimination from **2b** produces **4** in a process which is both kinetically feasible (i.e., with a relatively low unimolecular barrier of ca. 10 kcal/mol relative to **2b**) and thermodynamically favorable: The enthalpic driving force for this elimination is weak, around 0−2 kcal/mol (including bulk solvent effects via a polarizable continuum model), but is significantly increased for the free energies because of the gain in entropy. Thus, **2b** should not be stable in solution, where it would eventually decay to **4**. The computed chemical shifts are consistent with this interpretation; although the theoretical ^{51}V chemical shifts of **2b** and **4** are similar and are both compatible with experimental values, the $\delta(^{14}N)$ values of **2b** agree less well with experimental values than those of **4**.

Taken together, these results strongly suggest that the complex between aqueous vanadate and glycylglycine should be formulated as anionic, five-coordinated **4**. Earlier proposals based on static DFT computations, according to which the coordination geometry about vanadium in such complexes could be sensitive to the pH value,[11] are not supported by the present MD results: protonation of **4** would afford neutral, five-coordinate $[VO(OH)(GlyGly')]$ (**3**), not six-coordinate **1a**.

The combination of DFT-based MD simulations and NMR chemical shift calculations presents itself as a promising structural tool for the study of transition-metal complexes in aqueous solution. This combined approach can be used to assess structural details such as speciation and protonation state, with the main practical limitation that dynamic processes can be followed presently only on a short time scale of a few picoseconds.

Acknowledgment. The author wishes to thank Prof. Walter Thiel and the Max-Planck society for support. Computations were performed on a local computer cluster of Compaq XP1000, ES40, and Intel Xeon workstations and PCs at the MPI Mülheim and on an IBM regatta supercomputer at the Rechenzentrum Garching of the Max-Planck society.

Supporting Information Available: BP86/AE1 optimized coordinates of **1a,b**; **2b−d**; **4**; and **TS2b4**. This material is available free of charge via the Internet at http://pubs.acs.org.

IC050694I